Carbohydrate Research, 247 (1993) 129–144
Elsevier Science Publishers B.V., Amsterdam

Determination of proton–proton distances in 2-acetamido-2-deoxy monosaccharides from ^{1}H NMR relaxation measurements in solution

László Szilágyi [a,*] and Péter Forgó [b]

[a] *Chair of Organic Chemistry, L. Kossuth University, H-4010 Debrecen, P.O.B. 20 (Hungary)*
[b] *Chinoin Rt, H-1325 Budapest, P.O.B. 110 (Hungary)*

(Received December 22nd, 1992; accepted March 31st, 1993)

ABSTRACT

Determination of selective and biselective ^{1}H spin–lattice relaxation rates combined with steady-state and transient ^{1}H–^{1}H NOE data allowed calculation of intramolecular proton–proton distances in 2-acetamido-2-deoxy-D-glucosides (**1a** and **1b**), 2-acetamido-2-deoxy-D-mannoses (**5a** and **5b**) and their acetylated derivatives. These measurements were supplemented by DESERT studies using derivatives selectively labeled by ^{2}H at position 2. These distance data are in good correlation with literature values obtained by X-ray crystallography. Interproton distance measurements allow the determination of relative configurations, including that of the anomeric carbon, in hexopyranose rings in cases where other methods, like those based on scalar coupling constants, fail.

INTRODUCTION

Amino sugars are important constituents of cell-wall polysaccharides[1], glycoproteins[2], and antibiotics[3]. The diverse biological functions of these molecules are intimately related to their three-dimensional shapes determined, *inter alia*, by the conformations of the sugar rings and the glycosidic bonds. For glycoproteins, this statement refers, of course, only to the carbohydrate moiety of the molecule. It is well known, however, that carbohydrates attached to cell-surface proteins are crucial for cell recognition. Distortion of the sugar ring may also be involved in such biochemical processes as lysozyme catalysis (for a review, see ref 4).

Experimental determinations of pyranose ring conformations of saccharides in solution are generally based on the measurement of vicinal proton–proton (for a review see ref 5) or carbon-13–proton (for a review see ref 6) coupling constants. Interpretation of the data in terms of accurate torsional angles is not always straightforward despite considerable efforts invested in extending the scope of the

* Corresponding author.

Karplus relationship through improved parametrization[7–10]; this is especially true for vicinal $^{13}C-^{1}H$ coupling constants[11,12]. Some of the problems encountered in correlating three-bond coupling constants with conformations (torsional angles) are the following. (*a*) The experimental data basis is necessarily limited in terms of the range of torsional angles accessible within the chosen set[7]. (*b*) Parameters optimized for a particular set of reference compounds may (and, in general, do) give a poorer fit for experimental data obtained for a different group of structures[10]. (*c*) The reference torsional angles are usually obtained from X-ray data or as a result of empirical force field or semiempirical quantum chemical calculations. Evidently, solid-state (X-ray) or vacuum gas-phase values (calculations) cannot be considered as ideal references for data obtained *in solution* (NMR). It is desirable, therefore, to consider other NMR parameters related to conformation-dependent molecular quantities that are, unlike coupling constants, independent of the electron distribution details of the molecule investigated. Relaxation parameters (T_1, NOE) of nuclei coupled by dipolar interaction feature a strong dependence on internuclear distances (6th power) and are, therefore, promising in this respect. Conformational studies based on ^{1}H relaxation measurements have recently been published for carbohydrates[13] and other molecules[14]. Following an early summary[15], this field has been thoroughly reviewed[16]. 2-Acetamido-2-deoxy-D-glucose (GlcNAc) and its oligomers, $(GlcNAc)_n$, are known as inhibitors ($n = 1, 2, 3$) or substrates ($n > 3$) of hen egg lysozyme[17]. Other amino sugars, like 2-acetamido-2-deoxy-D-mannose (ManNAc), are also known to bind to lysozyme[17]. In order to determine the precise solution conformations of the monosaccharide inhibitors, we have measured selective and biselective spin–lattice relaxation times as well as steady-state and transient NOEs on **1a, 1b, 5a**, and **5b** in D_2O. These data are supplemented by DESERT[18] studies using derivatives selectively labeled at position 2 by ^{2}H: **2a, 2b, 6a**, and **6b**. Similar measurements have been performed on the acetylated derivatives **3a, 3b, 4a, 4b**, and **7b** in a nonpolar solvent (benzene). The solution data from these approaches will be compared with solid-state data obtained by X-ray crystallography for some of these or similar derivatives.

METHODS

Intramolecular dipole–dipole relaxation is the most important single source for NMR parameters directly related to internuclear distance. In the present study, we have made use of the following methods (cf. ref 16) to determine proton–proton distances.

NOE.—The cross-relaxation rate ($\sigma_{i,j}$), due to dipole–dipole interaction, between protons i and j bears a simple relationship to the distance, $r_{i,j}$, between them when extreme narrowing and isotropic molecular reorientation are assumed:

$$\sigma_{i,j} = \frac{1}{2} \frac{\gamma_H^4 \hbar^2}{r_{i,j}^6} \tau_c \qquad (1)$$

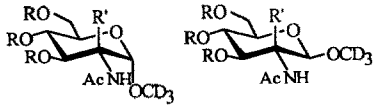

1a R=R' =H
2a R=H ; R'=D
3a R= Ac ; R' = H
4a R= Ac ; R' = D

1b R=R'=H
2b R=H ; R'=D
3b R=Ac ; R'=H
4b R=Ac ; R'= D

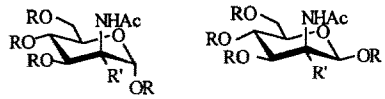

5a R=R'=H
6a R=H ; R'=D

5b R=R'=H
6b R=H ; R'=D
7b R=Ac ; R'=H

where τ_c is the rotational correlation time for the reorientation of the relaxation vector ($r_{i,j}$) and γ_H is the proton gyromagnetic ratio; $\sigma_{i,j}$ can be determined from NOE measurements in two ways. (*1*) The inital build-up rate of the NOE, as determined most conveniently in transient NOE (tr-NOE) experiments[19], is equal to $2\sigma_{i,j}$. (*2*) Steady-state NOEs also depend on $\sigma_{i,j}$ but, in multispin systems, they contain contributions from all dipolarly coupled nuclei to the relaxation of the observed spin (i):

$$f_i(j) = \frac{\sigma_{i,j}}{\sum_j \rho_{i,j}} = \frac{\sigma_{i,j}}{R^s_{1,i}} \qquad (2)$$

where $f_i(j)$ is the steady-state NOE value of spin i when j is saturated and $R^s_{1,i}$ is the total direct relaxation rate of spin i; this can be separately determined by measuring the selective spin–lattice relaxation rate[20,21] of i. Indirect effects[22] are neglected in (*2*).

Biselective T_1.—Separation of the cross-relaxation contribution of interest in multispin systems can also be accomplished by measuring the biselective relaxation rates[23,24], $R^{bi}_{i,j}$:

$$\sigma_{i,j} = R^{bi}_{i,j} - R^s_i \qquad (3)$$

Notice that measurements of NOEs or biselective T_1's both allow acquisition of two data sets for a particular $\sigma_{i,j}$ (hence, $r_{i,j}$); this, of course, enhances the accuracy of the distance to be determined. Practical difficulties, such as spectral overlap, may, however, limit exploitation of this possibility.

DESERT[18,25] (deuterium substitution effect on relaxation times).—The contribution of a particular proton k to the dipole–dipole relaxation of proton i can be conveniently measured through replacing k by another nucleus. When ^2H is used for this purpose, the steric and electronic structure of the molecule remains undisturbed for all practical purposes. The difference between the spin–lattice relaxation rates of i in the molecule without and with ^2H-substitution is:

$$\Delta R^0_{1,i} = R^0_{1,i} - \left(R^0_{1,i}\right)' \quad (4)$$

where the primed symbol refers to the molecule deuterated at position k and $R^0_{1,i}$ is the initial nonselective spin–lattice relaxation rate of proton i. Assuming, as before, extreme narrowing and isotropic reorientation,

$$R^0_{1,i} = \frac{4\gamma_i^2\gamma_k^2 \mathbf{I}_k(\mathbf{I}_k+1)\hbar^2}{3r^6_{i,k}}\tau_c$$

then:

$$\Delta R^0_{1,i} = \frac{3\gamma_H^4\hbar^2}{2r^6_{i,k}}\tau_c - \frac{8\gamma_H^2\gamma_D^2\hbar^2}{3r^6_{i,k}}\tau_c = 1.437\frac{\gamma_H^4\hbar^2}{r^6_{i,k}}\tau_c \quad (5)$$

taking into account that $\gamma_H/\gamma_D = 6.514$. Eqs *1–5* all contain the rotational correlation time which must be known beforehand in order to calculate internuclear distances. This problem is usually circumvented by relying on a "known" internuclear distance as a "molecular yardstick" against which unknown distances in the same molecule can be measured. Most often the C–H bond length (from X-ray measurements) is used for this purpose because it can be reasonably assumed not to change from molecule to molecule. It is generally assumed that, in a C–H fragment, the ^{13}C nucleus is relaxed practically exclusively by the dipolar mechanism through the proton directly bonded,

$$R_1(^{13}C) = N\frac{\gamma_H^2\gamma_C^2\hbar^2}{r^6_{C,H}}\tau_c \quad (6)$$

where N is the number of directly bonded hydrogens. Alternatively, proton–proton distances which can reasonably be assumed to remain constant in different molecules, such as those of geminal protons or protons in the *ortho*-position in aromatic rings, can also be chosen for the purpose of reference. Whichever method is chosen, it is essential to ensure that τ_c for the reference relaxation vector is identical with that of the proton pair in question. However, in the presence of internal motions, the correlation times calculated from ^{13}C and ^1H relaxation data may be different[26].

RESULTS AND DISCUSSION

The ^1H and ^{13}C NMR parameters of the compounds investigated are summarized in Table I. Relaxation and NOE data are collected in Tables II–V. Table VI

contains the proton–proton distances determined in this study as compared with X-ray data for model compounds from the literature. All distances derived from the relaxation data are referenced to the C–H bond length (1.08 Å) through measurement of ^{13}C spin–lattice relaxation times. Since T_1-values for ring carbons C-1 through C-5 are identical within experimental error (Table I), the assumption of isotropic rotational reorientation is justified in all cases considered here. It is also evident from these data that internal rotation of the CH_2OR (R = H, $COCH_3$) group at position 5 is considerably restricted in all cases, otherwise a much longer T_1 value should be observed for C-6. One of the most common structural problems with pyranose-ring sugars is concerned with the configuration of ring substituents, especially those at the anomeric (C-1) carbon. In the chair conformation, these are unambiguously portrayed by intraring H–H distances. Typical values, as estimated from molecular models, are:

Relative position	Distance (Å)
1,2-*eq* / *ax*	~ 2.40
1,2-*ax* / *ax*	~ 3.05
1,2-*eq* / *eq*	~ 2.60
1,3-*eq* / *ax*	~ 3.70
1,3-*ax* / *ax*	~ 2.60
1,3-*eq* / *eq*	~ 4.20
1,4-*eq* / *ax*	~ 4.10
1,4-*ax* / *ax*	~ 4.00
1,4-*eq* / *eq*	~ 5.10

It is clear from these figures that the relative orientations of protons in 1,2- or 1,3-positions in chair-shaped six-membered rings can be readily identified (with the possible exception of discriminating between 1,2-*eq* / *ax* and 1,2-*eq* / *eq*), provided the solution conformations are close to those in the solid state. For rigid systems like those studied here, this is a reasonable assumption as witnessed by previous examples[13,25] and by our data discussed below. Another prerequisite for the reliability of the structures derived from relaxation measurements is that the experimental error on distances should be small compared with the differences which discriminate one structure from the other. In the present case, differences of diagnostic value are in the range of ca. 0.4 to ca. 1 Å (except for 1,2-*eq* / *ax* vs. 1,2-*eq* / *eq* which cannot be distinguished safely, see above); therefore, an error of 0.1 to 0.2 Å (or 3 to 8% in relative terms) on the experimental distances seems to be acceptable for this purpose. Experimental errors from the measured relaxation parameters (T_1 and NOEs) are propagated into the calculated distances to an extent of only ca. 15% because of the sixth-root dependence. This is equal to a relative accuracy of ca. ±1.7% on the distances, assuming a conservative estimate of ±10% error on the measured parameters (further discussion below). Indeed, distances obtained for a particular proton pair from reciprocal experiments are often close to or better than this figure (Table VI). On the other hand, the error is larger (5–10%) when distance data derived from different types of experiments

TABLE I

^{1}H and ^{13}C NMR parameters of the compounds investigated

Compd	Solvent	Carbon chemical shifts (ppm) [^{13}C-T_1(s)]						τ_c[s] [b]	Proton chemical shifts (ppm) [$^{3}J_{H,H}$(Hz)]							Ref
		C-1	C-2	C-3	C-4	C-5	C-6		H-1 ($J_{1,2}$)	H-2 ($J_{2,3}$)	H-3 ($J_{3,4}$)	H-4 ($J_{4,5}$)	H-5 ($J_{5,6a}$)	H-6a ($J_{6a,6b}$)	H-6b ($J_{5,6b}$)	
1a	D_2O	99.1	54.5	72.5	70.8	72.0	61.4	4.3×10^{-11}	4.75	3.90	3.70	3.46	3.66	3.86	3.77	45
									(3.6)	(10.7)	(9.8)	(8.7)	(5.2)	(−12.3)	(2.0)	
1b	D_2O	102.7	57.9	74.8	70.8	76.7	61.6	4.7×10^{-11}	4.44	3.68	3.52	3.43	3.45	3.93	3.74	45
									(8.5)	(10.3)	(8.9)	(10.3)	(5.3)	(−12.3)	(1.5)	
3a	C_6D_6	99.7	53.3	72.8	69.9	69.2	63.29	4.0×10^{-11}	4.52	4.61	5.45	5.33	3.81	4.29	4.10	[a]
		(1.10)	(1.07)	(1.09)	(1.09)	(1.14)	(0.69)		(3.5)	(9.4)	(9.4)	(9.4)	(4.7)	(−12.2)	(2.7)	
3b	C_6D_6	101.4	55.2	72.7	69.4	72.2	62.1	4.3×10^{-11}	4.48	3.81	5.58	5.27	3.43	4.33	4.08	[a]
		(1.01)	(1.03)	(1.03)	(1.04)	(1.03)	(0.67)		(8.0)	(10.2)	(9.7)	(9.7)	(4.6)	(−12.2)	(2.5)	
5a	D_2O	95.7	55.9	71.5	69.5	74.7	63.2	4.0×10^{-11}	5.11	4.30	4.03	3.51	3.51			[a]
		(1.13)	(1.05)	(1.10)	(1.07)	(1.11)	(0.64)		(1.6)	(4.7)	(9.8)	(9.8)				
5b	D_2O	95.7	56.7	74.7	69.3	79.0	63.2	4.0×10^{-11}	5.01	4.43	3.80	3.61	3.40			[a]
		(1.13)	(1.06)	(1.06)	(1.12)	(1.11)	(0.65)		(1.7)	(4.5)	(9.6)	(9.6)	(4.9)			
7b	C_6D_6	91.14	50.1	72.1	65.5	73.7	61.9	5.3×10^{-11}	5.62	5.00	5.10	5.39	3.25	4.34	3.97	[a]
		(0.87)	(0.76)	(0.84)	(0.84)	(0.85)	(0.49)		(1.71)	(4.05)	(10.2)	(10.2)	(4.7)	(−12.6)	(2.3)	

[a] This study: ^{1}H spectral parameters obtained by first-order analysis, ^{13}C assignments from HMQC measurements. [b] Correlation times for **1a** and **1b** are from ref 46.

(Table VI) are compared. Such an accuracy is, however, still acceptable for the purpose of distinguishing between structural alternatives as discussed above. These methods are therefore complementary to NMR techniques currently in routine use for structure determination in the field of carbohydrates and may provide solutions to problems where conventional methods fail. For instance, determination of the anomeric configuration of pyranose-ring sugars is based conventionally on $^3J_{H\text{-}1,H\text{-}2}$ or $^1J_{C\text{-}1,H\text{-}1}$ values by way of the qualitative use[5] of the Karplus equation or other rules[27,28]. However, both approaches have well-known limitations. Thus, $^3J_{H\text{-}1,H\text{-}2}$ data are useful only when there is an axial proton at position 2 of the pyranose ring; when this proton is equatorial, distinction between anomers is no longer possible on this basis (e.g., sugars with *manno* configuration) and, trivially, there is

TABLE II

^{1}H relaxation data of methyl 2-acetamido-2-deoxy-D-glucosides and 2-acetamido-2-deoxy-D-mannoses [a]

Obsd proton	Compound	T_1^{ns}(s)	T_1^{s}(s)	NOE (%) [b] T_1^{bs}(s)				
				H-1	H-2	H-3	H-4	H-5
H-1	**1a(2a)**	2.27						
		(4.07)						
	1b(2b)	1.37	1.95		2.4	7.6		
	5a(6a)	4.59	5.78		25.1	1.7		
		(6.88)	(7.07)		*4.55*	(1.6)	(1.0)	
	5b(6b)	1.47	2.07		12.3			18.2
		(1.79)	(2.61)		*1.92*			(19.5)
H-2	**1b(2b)**	1.78	2.48					
	5a(6a)	2.50	3.37	17.1		23.5		
				2.80		*2.83*		
	5b(6b)	2.21	2.97	17.4				18.2
				2.62				*3.08*
H-3	**1a(2a)**	2.97		8.0				
		(3.82)						
	1b(2b)	1.45	1.97					
	5a(6a)	2.30	3.03	(0.9)	20.7		(3.9)	
		(3.58)	(4.15)	*2.98*	*2.52*			
H-4	**1a(2a)**	2.28						
		(3.79)						
	5a(6a)	3.38	(4.11)	(0.6)		(5.0)		
		(3.54)						
	5b(6b)	3.50						
		(3.66)						
H-5	**1a(2a)**	1.66						
		(1.74)						
	5a(6b)	1.30	1.91	16.8				
		(1.28)	(1.76)	(15.1)	*1.84*			
				1.59				

[a] Measured in D_2O at 308 K; values in parentheses are for the deuterated derivatives. [b] Steady-state values.

nothing to rely on in derivatives lacking hydrogen at position 2. Furthermore, it has been demonstrated[29] that, in certain cases, $^1J_{C\text{-}1,H\text{-}1}$ values may also not be relied upon for deducing the anomeric configuration. In contrast, distances between protons in 1,3-*ax*/*ax* and 1,3-*ax*/*eq* orientations in chair-shaped six-membered rings differ by at least 1 Å (see above), which should make distinction unambiguous in all practical cases (compare, e.g., $r_{1,3}$ or $r_{1,5}$ with $r_{3,5}$ in **3b, 4a, 6b**, and **7b**, Table VI).

In addition to using distance data for qualitative stereochemical assignments, it is of considerable interest to investigate the scope and limitations of the relaxation methods under discussion as an approach towards defining molecular geometry in solution quantitatively, very much as X-ray or neutron diffraction is used for solid-state structures. The errors arise basically from three sources: (*1*) the reliability of the reference distance (C–H or H–H) used for estimating rotational correlation times (see discussion under Methods); (*2*) approximations involved in the theoretical treatment (initial slope[30] approximation, neglect of multispin effects[21,22]); and (*3*) the accuracy of the relaxation parameters (T_1's and NOEs) measured. The first type of error should not be of great concern as long as only relative distances are considered, since this introduces approximately the same

TABLE III

^{1}H relaxation data of methyl 2-acetamido-3,4,6-tri-*O*-acetyl-2-deoxy-D-glucosides [a]

Obsd proton	Compound	T_1^{ns}(s)	T_1^{s}(s)	NOE (%) [b] $T_1^{bs}(s)$				
				H-1	H-2	H-3	H-4	H-5
H-1	**3a(4a)**	2.35				(1.6)	(1.1)	2.6 (3.1)
		(3.54)	(5.10)			*(4.27)*	*(4.79)*	*(4.14)*
	3b(4b)	1.15	1.67		2.8	5.8		16.9
		(1.24)			*1.56*	*1.52*	*1.73*	*1.40*
H-2	**3b(4b)**	1.94	2.44			3.9	10.1	
				2.17		*2.12*	*2.07*	*2.35*
H-3	**3a(4a)**	2.49	3.20					12.5 (13.6)
		(2.75)	(3.88)	*(3.36)*			*(3.38)*	*(3.16)*
	3b(4b)	1.69	2.22	7.7	3.6			9.7
		(1.93)		*2.08*	*2.13*		*2.17*	*2.06*
H-4	**3a(4a)**	2.79	3.47					6.0 (7.2)
		(3.92)	(5.47)	*(4.89)*		*(4.55)*		*(4.34)*
	3b(4b)	2.27	3.09		13.0			5.1
		(3.81)		*3.22*	*2.71*	*2.93*		*2.88*
H-5	**3a(4a)**	1.75	2.40			9.9 (11.1)	3.3 (3.5)	
		(1.82)	(2.70)	*(2.42)*		*(2.31)*	*(2.64)*	
	3b(4b)	1.07	1.51	14.3		6.4	2.7	
		(1.04)		*1.26*	*1.44*	*1.41*	*1.43*	

[a] Measured for solutions in C_6D_6 at 308 K; values in parentheses are for the deuterated derivatives.
[b] Steady-state values.

TABLE IV

^{1}H relaxation data for 2-acetamido-1,3,4,6-tetra-O-acetyl-2-deoxy-β-D-mannose (**7b**) [a]

Obsd proton	T_1^{ns}(s)	T_1^{s}(s)	NOE (%) [b] T_1^{bs}(s)						
			H-1	H-2	H-3	H-4	H-5	H-6a	H-6b
H-1	1.09	1.52		10.6	8.6		14.9		
				1.37	*1.38*	*1.53*	*1.32*		
H-2	1.52	1.95	11.4		14.9				
			1.71		1.71	*1.90*	1.95		
H-3	1.24	1.73	8.1				6.8		
			1.51	*1.51*		*1.67*	*1.59*		
H-4	1.90	2.31							
			2.30	*2.31*	*2.27*		*2.20*		
H-5	0.92	1.29	13.5						
			1.11	*1.31*	*1.23*	*1.27*			
H-6a	0.55	0.86							32.9
									0.61
H-6b	0.58	0.88						32.7	
								0.64	

[a] Measured for solutions in C_6D_6 at 296 K. [b] Steady-state values.

systematic error in all distance values to be compared. Let us now consider the error arising from neglecting the indirect ("three spin") effect in eq *2*. This can, in general, lead to severe errors in distance determination if not properly accounted for[31]; in the present examples, however, noticeable deviations were not detected. A case in point is **3b** where the steady state NOE at H-1 is large (16.9%) when H-5 is irradiated and small (5.8%) when H-3 is the target of irradiation (Table III). Since the three axial protons concerned form a triangle, operation of indirect effects is to be expected. These have been discussed[21] in detail in connection with a closely analogous structure. The exact three-spin formula[21,22] for this particular case is

$$\frac{r_{1,5}^6}{r_{1,3}^6} = \frac{\sigma_{1,3}}{\sigma_{1,5}} = \frac{f_1(3) + f_5(3) f_1(5)}{f_1(5) + f_3(5) f_1(3)}. \qquad (7)$$

Using enhancements from Table III, eq *7* gives $r_{1,3}/r_{1,5} = 1.169$. This value has to be contrasted with $2.66/2.25 = 1.182$ calculated from distances (Table VI) obtained by neglecting indirect effects (eq *2*). The possible error in distances is less than 2% in this case, which is particularly favorable for the operation of indirect effects in steady-state NOE measurements. Concerning measurement accuracies, it is to be noted that results based on eq *2* are affected by errors both in NOE and T_1 measurements. Transient NOE therefore appears more attractive, especially because the cross-relaxation rate is twice that obtained in steady-state NOE (or in TOE[32]) experiments. These advantages are, however, offset by the smaller maximum enhancement in the extreme narrowing limit (38.5%)[33] and by the need to take data from the initial (linear) portion of the build-up curve where enhance-

TABLE V

Cross-relaxation rates from transient NOE experiments

Compound	Inverted proton (i)	Observed proton (j)	$\sigma_{i,j}(s^{-1})$
1b	1	3	0.045
	3	1	0.061
3a	3	5	0.061
	5	3	0.054
4b	1	3	0.030
	1	5	0.071
	3	1	0.026
	3	2	0.017
	3	5	0.042
	4	2	0.026
	5	1	0.064
	5	3	0.036
5a	1	2	0.050
	2	1	0.053
	2	3	0.094
5b	1	2	0.054
	2	1	0.060
	1	5	0.080
6b	1	5	0.101
	1	3	0.051
	5	1	0.106
	5	3	0.039
7b	1	2	0.062
	1	5	0.094
	2	1	0.066
	3	1	0.055
	5	1	0.096

ments are necessarily far from the maximum values. From typical build-up curves (Fig. 1), it is apparent that the practical upper limit to distance determination by this method is ~ 3 Å in small molecules. Measurements of biselective relaxation rates (eq *3*) or DESERT (eq 5), on the other hand, share the common technical drawback that cross-relaxation rates which are small relative to $(T_1)^{-1} = R_1$ are obtained by taking the difference between two R_1's. With errors around $\pm 5\%$ in T_1 measurements, the error in small cross-relaxation rates may easily go up to 100% or more. As a practical example, let us consider two protons ~ 3 Å apart in a molecule reorienting with a rotational correlation time of 4×10^{-11} s. Eq *1* then predicts a cross-relaxation rate of 0.017 s^{-1}, which is $\sim 5\%$ of R_1^{bi} or R_1^s corresponding to T_1^{bi} or $T_1^s \sim 3$ s. Since the experimental error in the latter is similar in magnitude to the quantity $(\sigma_{i,j})$ directly related to the internuclear distance, the correct interpretation of the above data is that $r_{i,j} > 2.8$ Å (this particular value corresponds to $\sigma_{i,j} = 0.034$ s^{-1}, i.e., a 100% error was assumed).

TABLE VI

Comparison of H · · · H distances determined by different methods

Compd	Method [a]	H · · · H distance (Å)									Ref
		r_{12}	r_{13}	r_{15}	r_{23}	r_{24}	r_{34}	r_{35}	r_{45}	$r_{6a,6b}$	
1a(2a)	D	2.35			2.75	2.39					
	X	2.68	3.75	3.61	2.92	2.68	2.82	2.61	2.82	1.67	41
	X	2.38	3.73	3.62	2.83	2.55	2.86	2.51	2.87	1.61	42
	X	2.43	3.80	3.70	3.07	2.44	3.06	2.38	3.08	1.87	43
1b	N	3.18	2.59								
			2.61								
	T		2.45								
			2.55								
	X	2.95	2.51	2.31	2.87	2.63	2.85	2.58	2.99	1.56	41
3a(4a)	N		(3.90)	(3.50)				2.55 (2.55)	2.94 (3.08)		
								2.57 (2.62)	3.06 (3.09)		
	D	2.47			3.08	2.61					
	T							2.43			
								2.39			
3b(4b)	N	3.01	2.66	2.23	3.03	2.58		2.56	3.01		
			2.66	2.25	3.03	2.59		2.58	2.98		
	B		2.73	2.18				2.65			
			2.43	2.00				2.57			
	D	2.86			2.80	2.42					
	T		(2.70)	(2.33)	(2.96)	(2.75)		(2.55)			
			(2.75)	(2.37)				(2.61)			
5a(6a)	N	2.53	(4.12)		2.34		(3.26)				
		2.46	(4.16)		2.34		(3.12)				
	B	2.50			2.36						
		2.40			2.42						
	D	2.68			2.36	3.70					
	T	2.47			2.22						
		2.45									
5b(6b)	N	2.40		2.24							
		2.40		2.24							
				(2.22)							
				(2.28)							
	B	2.51		2.33							
		2.58		2.18							
	D	2.32				3.74					
	T	2.44	(2.46)	2.28				(2.57)			
		2.40		(2.19)							
				(2.18)							
	X	2.29	2.43	2.36	2.31	3.64	2.83	2.50	2.82	1.57	44
7b	N	2.44	2.52	2.30	2.40			2.59		1.84	
		2.51	2.56	2.28						1.84	
	B	2.44	2.44	2.28	2.43			2.56		1.79	
		2.40	2.35	2.21	2.35			2.76		1.77	
	T	2.48	2.54	2.32							
		2.46		2.30							

[a] N, from eqs *1* and *2*; B, from eqs *1* and *3*; T, eq *1* through transient NOE measurement; D, DESERT eq *5*; X, X-ray data.

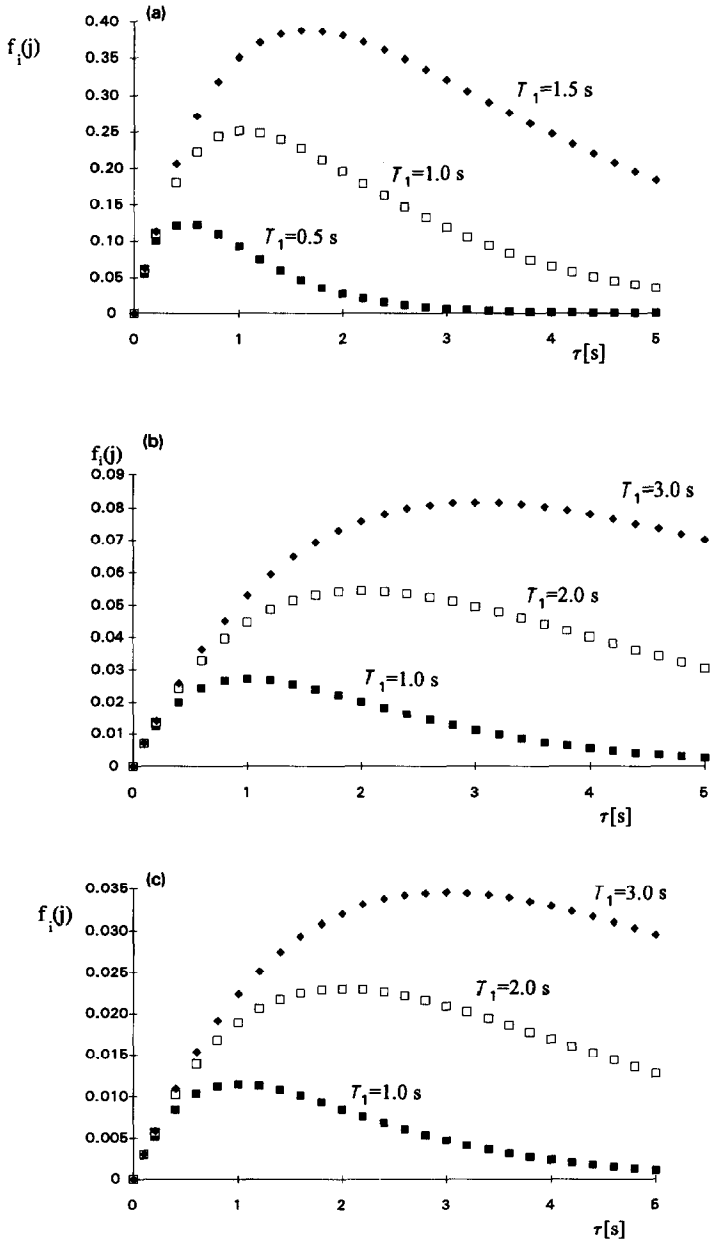

Fig. 1. Development of transient NOEs, $f_i(j)$, calculated according to eq 4.10 in ref 33 for proton pairs separated by distances characteristic for (a) geminal ($r_{i,j} = 1.8$ Å), (b) 1,3-diaxial ($r_{i,j} = 2.6$ Å), and (c) 1,2-diaxial ($r_{i,j} = 3.0$ Å) positions in six-membered chair rings, $\tau_c = 4 \times 10^{-11}$ s. $T_{1,i}$ was assumed to be equal to $T_{1,j}$ and the calculations have been performed for three different values, indicated on the curves, of this parameter.

The situation is slightly better for DESERT measurements since the pertaining relaxation rate differences (ΔR, eq *5*) are ca. three times larger than those in eq *3*. These correlations are summarized in Fig. 2.

In Table VI, we have listed X-ray data for structures closely similar to those investigated here. The correlation between solution and solid-state distances is fairly satisfactory, especially for values up to ~ 3 Å as demonstrated in Fig. 3. It is also evident from the data in Table VI that free (**1**, **2**, **5**, and **6**) and acetylated (**3**, **4**, and **7**) derivatives in polar and apolar solvents, respectively, do not show any appreciable conformational differences at least to the extent of exceeding the limits of experimental accuracy.

Finally, some points of practical interest need to be addressed. All methods, except DESERT, used in this study require selective perturbation of resonances; spectral overlap is therefore the single most serious limitation against general use. Increased access to high-field spectrometers, exploitation of solvent effects for enhancing spectral dispersion, and application of shaped pulses for selective excitation[34] may alleviate this problem. Selective methods are, however, likely to remain useful for the study of small molecules where complete or almost complete sets of accurate distance data will be accessible or else, with larger molecules, where some distances may be acquired at high precision depending on spectra. An added restriction with eqs *2* and *3* is that resonances of both nuclei involved in the distance measurement must be accessible to selective perturbation, whereas, in the transient NOE experiment, the observed resonance may be overlapped by others. This technique seems therefore to be the most attractive and generally useful one but, unfortunately, it has serious sensitivity problems as discussed above. NOESY,

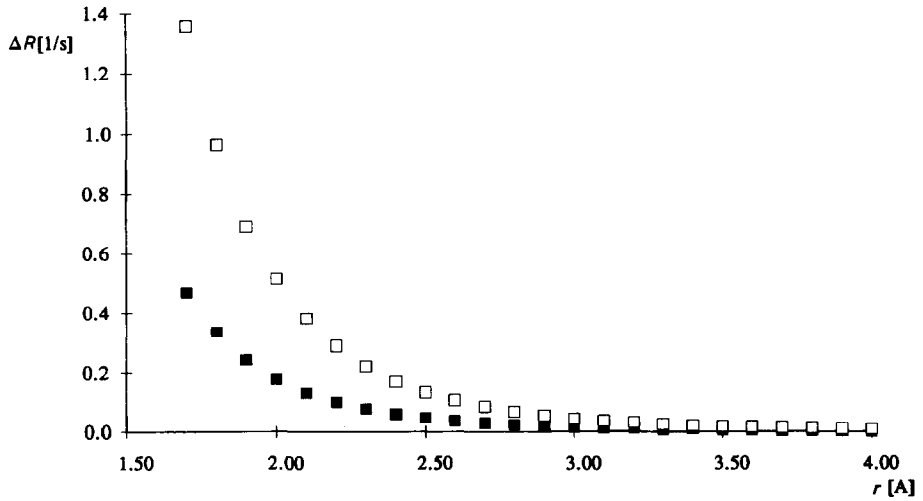

Fig. 2. Dependence of measured relaxation parameters, $\Delta R^0_{i,i}$ and $\sigma_{i,j}$, on H···H internuclear distances ($r_{i,j}$) in DESERT (eq *5*, □) and biselective relaxation time (eq *3*, ■) measurements, respectively.

the 2D analogue of the transient NOE experiment, largely overcomes the overlap problems, but lags behind 1D methods in terms of accuracy and presents special problems when applied to small molecules[35]. DESERT is attractive for its experimental simplicity and less stringent requirements for spectral dispersion, but it is obviously restricted by the need for specific ^{2}H-substitution which may limit its use mainly to the measurement of distances to exchangable protons[18,36] like OH and NH. When complete sets of accurate distances are needed for precise definition of molecular geometry in solution, it is desirable to attack the problem by multiple techniques, partly because multiplying the data for a particular distance is likely to enhance the reliability of the measurement. On the other hand, different methods may provide complementary information as demonstrated here in the case of **4a** where $r_{1,2}$, $r_{2,3}$, and $r_{2,4}$ could only be determined by DESERT, whereas the other distances listed were obtained mainly by NOE/selective T_1 measurements and were inaccessible, for obvious reasons, by DESERT.

EXPERIMENTAL

The syntheses of the compounds used in this study have been described previously[37]. All ^{1}H (400 MHz) and ^{13}C (100 MHz) measurements were performed on a Bruker AC 400-P instrument on 0.01 M solutions in D_2O (**1a, 1b, 2a, 2b, 5a, 5b, 6a**, and **6b**) or benzene-d_6 (**3a, 3b, 4a, 4b**, and **7b**) in 5-mm tubes. The samples were thoroughly degassed by at least four freeze–pump cycles and then sealed under vacuum. For the solutions in D_2O, degassing was performed in a separate container, to prevent sample tube cracking, and then transferred into the sample

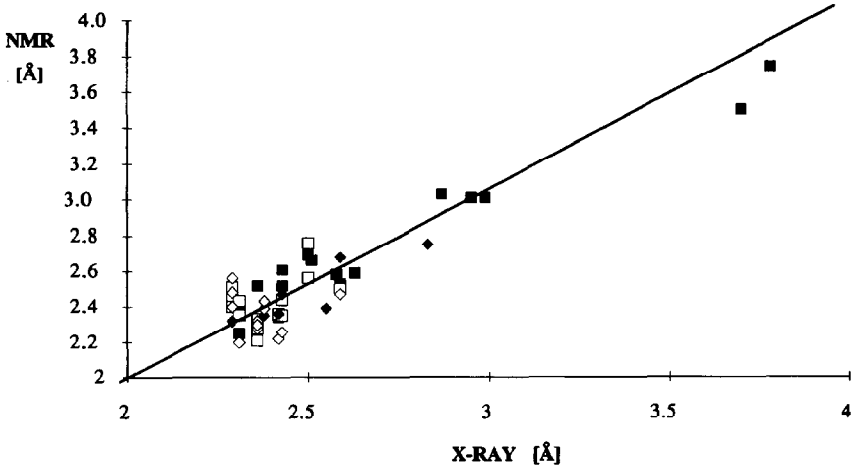

Fig. 3. Correlation between H···H distances determined by X-ray crystallography and NMR relaxation measurements (Table VI) using eqs *1* (◇), *2* (■), *3* (□), and *5* (◆). In cases when more than one set of X-ray data was available for the same proton pair, the arithmetic mean value was taken as the reference X-ray distance. The correlation coefficient for the linear fit is 0.97.

tubes under Ar before evacuation and sealing. The probe temperature was set to either 296 ± 1 K (for **3b, 4b**, and **7b**) or 308 ± 1 K (for **1, 2, 3a, 4a, 5**, and **6**) using the B-VT 1000E temperature accessory. The use of different temperatures for different samples was dictated by the need to ensure that the NH-signal of the acetamido group does not overlap with resonances of interest. All measurements, including ^{13}C T_1 determination, for a particular sample were, of course, made at the same temperature. Steady-state NOE values were determined with a preirradiation time of ≥ 5 T_1^{ns}(max) as described previously[38]. Typically, 200–300 scans were accumulated into 16 K data points for each saturated multiplet for spectral widths of 3000 Hz. In order to improve integration accuracy, the number of data points was increased to 32 K by zero-filling before exponential multiplication (LB = 1.0 Hz) and FT. ^1H (nonselective and selective) and ^{13}C T_1 determinations were performed by the inversion–recovery method. Selective inversion pulses were generated by the DANTE[39] sequence using the transmitter operated in the low-power mode (TLO). The 90° pulse length was 90 μs in the TLO mode. The DANTE pulse interval was adjusted according to the requirements of selectivity and avoidance of unwanted excitation by side-band frequencies, usually between 0.25–0.40 ms. The 180° selective pulses were made up of 90 component pulses, resulting in a total duration of 20–30 ms. For the biselective relaxation measurements, two selective 180° pulses were given in succession at the resonance frequencies of the target multiplets. The 90° "read" pulses were always "hard" pulses (6 μs) derived from the main ^1H-transmitter (THI). Proton T_1-values were calculated with the aid of Bruker's T_1 routine from spectra taken for 8–10 variable τ-values such that $\tau_{max} < T_1$ (initial rate approximation). The rotational correlation times (Table I) were obtained (eq *6*) from the average of T_1-values for C-1 to C-5 for each compound in Table I. Cross-relaxation rates from transient NOE measurements (Table V) were determined following the suggestion of ref 40. First, an approximate build-up curve was determined using relatively small number of scans; then, one or two τ-values were selected at the initial linear portion of the curve and the experiment was repeated with a much better S/N for obtaining reliable enhancement values. The cross-relaxation rate was then taken equal to $\mathrm{tg}\alpha$ where α is the angle subtended by the straight line drawn from the origin of the coordinate axes (enhancement vs. τ, see Fig. 1) to the points of measurement.

ACKNOWLEDGMENTS

This work was supported by a grant, OTKA T4023 (to L. Sz.), from the Hungarian National Science Fund. We thank Dr. B. Podányi (CHINOIN Rt., Budapest) for his interest and advice.

REFERENCES

1 G. Baschang, *Tetrahedron*, 45 (1989) 6331–6360.
2 H. Kessler, H. Matter, G. Gemmecker, A. Kling, and M. Kottenhahn, *J. Am. Chem. Soc.*, 113 (1991) 7550–7563.

3 J. Bérdy, A. Aszalós, M. Bostian, and K.L. McNitt (Eds.), *CRC Handbook of Antibiotic Compounds*, Vol. 1, CRC Press, Boca Raton, FL, 1980, pp 105–121.
4 C.B. Post, C.M. Dobson, and M. Karplus, *ACS Symp. Ser.*, 430 (1990) 377–388.
5 K. Bock and H. Thogerson, *Annu. Rep. NMR. Spectrosc.*, 13 (1982) 2–57.
6 P.E. Hansen, *Progr. Nucl. Magn. Reson. Spectrosc.*, 14 (1981) 175–295.
7 L.A. Donders, F.A.A.M. de Leeuw, and C. Altona, *Magn. Reson. Chem.*, 27 (1989) 556–563.
8 E. Diez, J. San-Fabián, J. Guilleme, C. Altona, and L.A. Donders, *Mol. Phys.*, 68 (1989) 49–63.
9 M. Barfield and W.B. Smith, *J. Am. Chem. Soc.*, 114 (1992) 1574–1581.
10 K. Imai and E. Osawa, *Tetrahedron Lett.*, 30 (1989) 4251–4254.
11 F.H. Cano, C. Foces-Foces, J. Jiménez-Barbero, A. Alemany, B. Bernabé, and M. Martín-Lomas, *J. Org. Chem.*, 52 (1987) 3367–3372.
12 I. Tvaroška, M. Hricovíni, and E. Petráková, *Carbohydr. Res.*, 189 (1989) 359–362.
13 P.C. Kline, A.S. Serianni, S.-G. Huang, M. Hayes, and R. Barker, *Can. J. Chem.*, 68 (1990) 2171–2182.
14 A. Sega, M. Ghelardoni, V. Pestellini, L. Pogliani, and G. Valensin, *Magn. Reson. Chem.*, 22 (1984) 649–652; T. Sai, N. Takao, and M. Sugiura, *ibid*, 30 (1992) 1041–1046.
15 L.D. Hall, *Chem. Soc. Rev.*, 4 (1975) 401–420.
16 P. Dais and A.S. Perlin, *Adv. Carbohydr. Chem. Biochem.*, 45 (1987) 125–168.
17 T. Imoto, L.N. Johnson, A.C.T. North, D.C. Phillips, and J.A. Rupley, in P. Boyer (Ed.), *The Enzymes*, 3rd ed., Academic, New York, 1972, pp 665–868.
18 K. Akasaka, T. Imoto, S. Shibata, and H. Hatano, *J. Magn. Reson.*, 18 (1975) 328–343.
19 S.L. Gordon and K. Wüthrich, *J. Am. Chem. Soc.*, 100 (1978) 7094–7096.
20 D. Kaplan and G. Navon, *J. Chem. Soc., Perkin Trans. 2*, (1981) 1374–1383.
21 R. Freeman, H.D.W. Hill, B.L. Tomlinson, and L.D. Hall, *J. Chem. Phys.*, 61 (1974) 4466–4473.
22 J.H. Noggle and R.E. Schirmer, *The Nuclear Overhauser Effect*, Academic, New York, 1971.
23 L.D. Hall and H.D.W. Hill, *J. Am. Chem. Soc.*, 98 (1976) 1269–1270.
24 L.D. Hall, K.F. Wong, and H.D.W. Hill, *J. Chem. Soc., Chem. Commun.*, (1979) 951–953.
25 L.D. Hall, K.F. Wong, W.E. Hull, and J.D. Stevens, *J. Chem. Soc., Chem. Commun.*, (1979) 953–955.
26 M. Hricovíni, R.N. Shah, and J.P. Carver, *Biochemistry*, 31 (1992) 10018–10023.
27 A.S. Perlin and B. Casu, *Tetrahedron Lett.*, (1969) 2921–2924.
28 K. Bock and C. Pedersen, *J. Chem. Soc., Perkin Trans. 2*, (1974) 293–297.
29 L. Szilágyi and Z. Györgydeák, *Carbohydr. Res.*, 143 (1985) 21–41.
30 R. Freeman, S. Wittekoek, and R.R. Ernst, *J. Chem. Phys.*, 52 (1970) 1529–1544.
31 J.P. Carver and D.A. Cumming, *Pure Appl. Chem.*, 59 (1987) 1465–1476.
32 G. Wagner and K. Wüthrich, *J. Magn. Reson.*, 33 (1979) 675–680.
33 D. Neuhaus and M. Williamson, *The Nuclear Overhauser Effect in Structural and Conformational Analysis*, VCH, New York, 1989.
34 H. Kessler, S. Mronga, and G. Gemmecker, *Magn. Reson. Chem.*, 29 (1991) 527–557.
35 N.H. Andersen, H.L. Eaton, and X. Lai, *Magn. Reson. Chem.*, 27 (1989) 515–528.
36 C. Rossi and N. Marchettini, *J. Magn. Reson.*, 93 (1991) 614–617.
37 L. Szilágyi, P. Herczegh, and Gy. Bujtás, *Z. Naturforsch., Teil B*, 32 (1977) 296–298.
38 L. Szilágyi, *Carbohydr. Res.*, 170 (1987) 1–17.
39 G.A. Morris and R. Freeman, *J. Magn. Reson.*, 29 (1978) 433–462.
40 M. Clore and A.M. Gronenborn, *J. Magn. Reson.*, 61 (1985) 158–164.
41 F. Mo and L.H. Jensen, *Acta Crystallogr., Sect. B*, 34 (1978) 1562–1569.
42 F. Mo and L.H. Jensen, *Acta Crystallogr., Sect. B*, 31 (1975) 2867–2873.
43 L.N. Johnson, *Acta Crystallogr.*, 21 (1966) 885–891.
44 A. Neuman, H. Gillier-Pandraud, and F. Longchambon, *Acta Crystallogr., Sect. B*, 31 (1975) 2628–2631.
45 S.J. Perkins, L.N. Johnson, D.C. Phillips, and R.A. Dwek, *Carbohydr. Res.*, 59 (1977) 19–34.
46 L. Szilágyi and P. Forgó, *Biophys. Chem.*, 40 (1991) 89–96.